ELSEVIER

Thermochimica Acta 351 (2000) 55–60

thermochimica acta

www.elsevier.com/locate/tca

Thermal decomposition study of erbium oxalate hexahydrate

Basma A.A. Balboul

Chemistry Department, Faculty of Science, Minia University, El-Minia 61519, Egypt

Received 28 September 1999; received in revised form 16 December 1999; accepted 17 December 1999

Abstract

The thermal decomposition of erbium oxalate hydrate ($Er_2(C_2O_4)_3{\cdot}6H_2O$) till 900°C, in air and nitrogen, is investigated by nonisothermal gravimetry and differential thermal analyses. The activation energy (ΔE) is determined for each thermal decomposition step. The gaseous decomposition products are identified by infrared (IR)-spectroscopy. Intermediate and final solid products are characterized by IR-spectroscopy and X-ray diffraction (XRD). The results indicate that, in air atmosphere, following a stepwise dehydration at 90–370°C, the anhydrous product was noncrystalline and thermally unstable. An oxycarbonate $Er_2O_2CO_3$ is obtained at 450°C which decomposes near 600°C into crystalline Er_2O_3. The atmosphere has no affect on the decomposition pathway. The oxide proportion and crystallinity improved on increasing the temperature to 800°C. The volatile decomposition products were water vapor and carbon oxides.

Keywords: Er-oxalate; Er-oxide; Decomposition; DTA; TG; IR; XRD

1. Introduction

Characterization of the course of thermal decomposition enables the provision of adequate thermal conditions for producing a solid having specific properties. For instance, sintering must be avoided if an oxide is to be used as a catalyst or catalyst support [1–3], since in catalysis, materials of high surface area are required [2]. In contrast, metal oxides to be used as refractory materials must exhibit thermal resistance and mechanical stability [3,4]. Sintering of solid particles should therefore be enhanced.

The thermal behavior of transition metal oxalates has been investigated thoroughly [1–3]. However, rare earth metal oxalates have received much less attention, with little agreement on decomposition temperature, nature and stability of the intermediates, and the stoichiometry of the final oxide product [5].

Erbium sesquioxide, Er_2O_3, has a cubic structure below 2280°C. At higher temperatures, it transforms into a hexagonal structure [4]. The cubic structure of Er_2O_3 has been used as a catalyst in the dehydration of alkan-2-ols to alk-1-enes and for the oxidative coupling of methane as a petrochemical industrial catalyst [6,7]. Er_2O_3 is a basic oxide whose basicity and catalytic properties are dependent on the method of preparation and pretreatment [7]. There is no information available in the literature about the thermal decomposition of Er-oxalate compared to other rare earth metal salts. The decomposition of the basic carbonate dihydrates, $Er_2(OH)_2(CO_3)_2{\cdot}2H_2O$ was studied by Giolito et al. [8]. They reported that the first

PII: S0040-6031(00)00353-1

mass loss, observed between 33 and 200°C, is due to the formation of unhydrated basic carbonate $Er_2(OH)_2(CO_3)_2$. Final decomposition started immediately after dehydration through a slow process, completed at 650°C with the formation of Er_2O_3 as a final product. As in the case of Ho-basic carbonate, the intermediates, $Er_2O_2CO_3$ and/or $Er_2O_{2+x}(CO_3)_{1-x}$, were not detected.

Brzyska and Krol [9] studied the thermal decomposition of $Er_2(C_{10}H_8O_6)_3{\cdot}7H_2O$ (benzene-1,4-dioxyacetate ion) in air. They reported that, after complete dehydration, final decomposition occurred immediately via a slow process and was completed at 820°C to form Er_2O_3. No stable intermediates were reported. In contrast, Murasihi et al. [10] reported that, during the decomposition of Er-malonate in N_2 atmosphere, $Er_2O_2CO_3$, oxycarbonate was formed as an intermediate at 238°C. Er_2O_3 was formed at 652°C. Brzyska and Sikorska [11] studied the decomposition of Er-urate penta hydrate complex ($Er(C_5H_3N_4O_3)_3{\cdot}5H_2O$). They reported that complete dehydration occurs at 230°C. Er_2O_3 was formed at 675°C and no $Er_2O_2CO_3$ was formed as an intermediate. Hussein [12] studied the thermal decomposition of praseodymium oxalate hydrate in different atmospheres of gases (air, N_2, O_2). It was reported that the intermediates and final solid products are the same in air or in N_2 atmosphere. The thermal steps and the composition of the solid products are also the same in oxygen but shifted to lower temperature, i.e. oxygen gas only accelerated the decomposition steps.

The present study attempts to characterize the thermal decomposition of $Er_2(C_2O_4)_3{\cdot}6H_2O$ to the onset of Er_2O_3 by means of thermogravimetry (TG) and differential thermal analysis (DTA). The gaseous decomposition products were analyzed by means of infrared (IR)-spectroscopy. The solid products of the reaction were analyzed by IR-spectroscopy and X-ray diffractometry. The activation energy, ΔE, of the observed thermal processes is obtained by the non-isothermal method of thermanalytical data analysis.

2. Experimental

2.1. Material

$Er_2(C_2O_4)_3{\cdot}6H_2O$, abbreviated as ErOx (99.9%), was obtained from Wako Pure Chemical Industry, Japan. The calcination products were obtained by heating at various temperatures (200–800°C) for 1 h in air. The calcination temperatures were chosen on the basis of the thermal analysis data. For simplicity, these products are denoted in the text by ErOx, followed by the calcination temperature. Thus, ErOx800 represents decomposition products of ErOx at 800°C for 1 h. The abbreviation ML stands for mass loss.

2.2. Thermal analysis

Thermal analysis was performed using a DuPont 9900 Model DTA 951-TG 910 (USA). TG and DTA curves were recorded till 800°C at different heating rates (5–20°C/min) in air and N_2 (50 ml/min). Equal masses of the test sample (ca. 15 mg) were used in TG measurements. Highly sintered α-Al_2O_3 was used as the reference material for the DTA measurements.

The temperatures ($T_{\max}$) at which weight-variant (DTG) thermal processes are maximized were determined as a function of the heating rate (θ).

The activation energy (ΔE, kJ/mol) was then calculated for each thermal process from plots of log θ against $1/T_{\max}$ according to the following relationship [13]:

$$\Delta E = -\frac{R}{bd\log\theta\, d}\left(\frac{1}{T_{\max}}\right) \qquad (1)$$

where R is the gas constant (8.314 J/mol K) and b is a unitless constant (0.457).

2.3. Infrared (IR)-spectroscopy

1. IR-spectra were obtained at a resolution 4 cm^{-1}, between 4000 and 400 cm^{-1}, using a model FT/IR 410 JASCO (Japan). IR-spectra of ErOx and its solid calcination products were obtained from thin (<20 mg/m^2), lightly loaded (<1%) KBr-supported discs.
2. IR-identification of the gaseous decomposition products was done with the help of spectra (4000–600 cm^{-1}) taken for the gas surrounding a 0.5 g sample of ErOx heated at 10°C/min to various temperatures (100–450°C) for 5 min, in a specially designed IR-cell described elsewhere [14]. The cell was equipped with KBr windows, and

evacuated to 10^{-3} Torr for 5 min prior to recording the gas phase spectra. The cell background spectrum was then subtracted.

2.4. X-ray diffraction (XRD)

XRD powder patterns were obtained using a JSX-60P JEOL diffractometer equipped with a Ni-filter and Cu Kα radiation (λ=1.5418 Å). The operational settings for all the XRD scans were voltage: 40 kV; current: 30 mA, range 4–60° 2θ, scanning speed: 8°/min, slit width: 0.02°. For identification purposes, the relative intensities (I/I^0) and the d-spacings (Å) were compared with standard patterns of the ASTM powder diffraction files [15].

3. Results and discussion

TG and DTA curves in air or nitrogen (Fig. 1) reveal six mass loss (ML) processes (designated I–VI) in the decomposition of ErOx ($Er_2(C_2O_4)_3{\cdot}6H_2O$). In air, two of these (Processes IV, T_{max}=420°C and V, T_{max}=450°C) are exothermic, whereas the others are endothermic. The ML effected via the first two processes (I and II) accounts for a stepwise dehydration of ErOx·$6H_2O$, in which, Process I (ML=7.9%, T_{max}=90°C) involves the elimination of $3H_2O$ and Process II (ML=10.3%, T_{max}=150°C) leads to the removal of 1 mol of H_2O, with the formation of ErOx·$2H_2O$. The corresponding activation energies (Table 1) are well within the range (<60 kJ/mol) for removal of weakly bound water of crystallization from analogous compounds [3]. The ErOx·$2H_2O$ thus formed persists upon further heating to 315°C, the temperature at which Process III (T_{max}=360°C) commences operation. The total ML effected at 380°C (ca. 15.6%) accounts for elimination of the remaining $2H_2O$, and consequently, for the formation of an anhydrous product (presumably Er-oxalate). The energy of activation calculated for Process III (ΔE=105 kJ/mol) is indicative of a less facile removal of water from the dihydrate than from the hexahydrate (ΔE<45 kJ/mol).

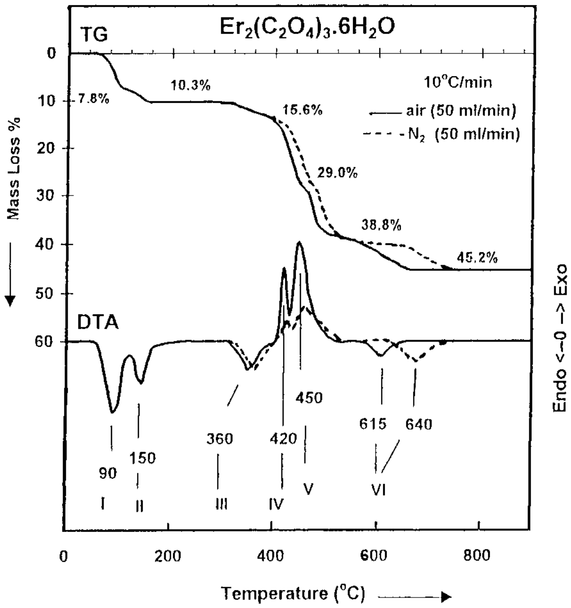

Fig. 1. TG and DTA curves recorded for ErOx at the heating rates indicated in dynamic air and nitrogen atmospheres.

Table 1
Activation energy (ΔE) values calculated for the thermal processes monitored in Fig. 1

Process	ΔE (kJ/mol)
I	42
II	45
III	105
IV	119
V	111
VI	160

In support of the above results, the IR-gas-phase spectra at 150 and 300°C (Fig. 2) display only a broad absorption centered around 3420 cm^{-1} and a strong absorption at 1650 cm^{-1} due to (νOH) and (δHOH) vibrations, respectively, of water molecules [16,17].

The IR-spectrum obtained for ErOx-200 (Fig. 3) is similar to that exhibited by the untreated ErOx·$6H_2O$ in displaying almost all of the characteristic absorptions of the oxalate anions (at 1750–640 cm^{-1}) and water of hydration 3449 and 1640 cm^{-1}) [16,17].

XRD analysis of ErOx-200 (Fig. 4) gives rise to a diffraction pattern identical to that documented (ASTM No. 32-1443) for ErOx·$2H_2O$.

Upon further heating, Process III is overlapped by a rapid exothermic ML process (Process IV,

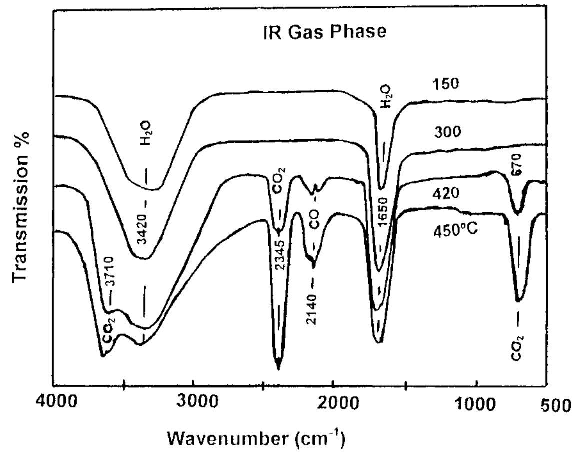

Fig. 2. IR-gas-phase spectra recorded from the gas surrounding 20 mg of ErOx at the temperatures indicated.

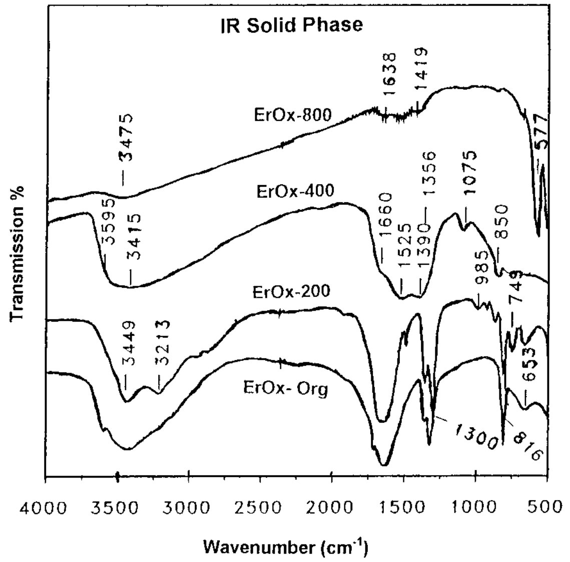

Fig. 3. IR-spectra of ErOx and its calcination products at the temperatures indicated.

T_{max}=420°C) and (Process V, T_{max}=450°C). The ML for Process IV is 29.0% which is close to that expected (28.6%) for the formation of $Er_2(CO_3)_3$, as follows:

$$Er_2(C_2O_4)_3 \rightarrow Er_2(CO_3)_3 + CO + CO_2$$

In support, at 420°C, the IR-gas-phase spectrum in Fig. 2 shows a slight increase in the water absorptions and the appearance of characteristic bands of CO_2 (at 2345 and 670 cm^{-1}) and CO (at 2140 cm^{-1}) [17,18]. This is consistent with rapid decomposition of ErOx following the dehydration process.

Process V slows down markedly near 500°C (Fig. 1), amounting to a total ML of ca. 38.8%, which

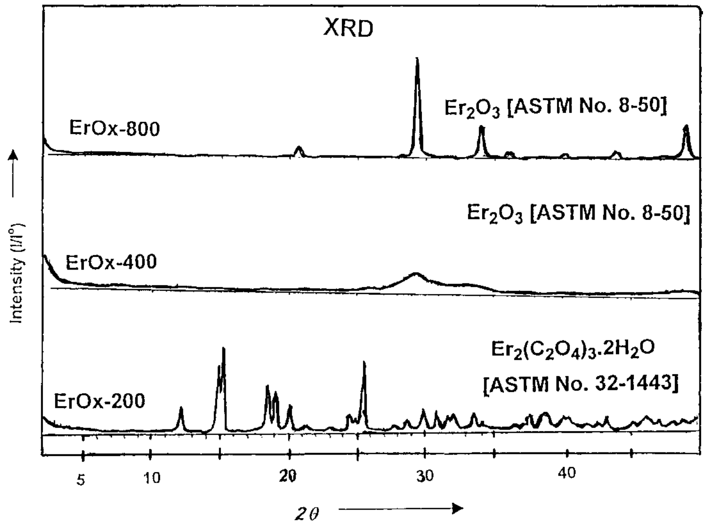

Fig. 4. X-ray powder diffractograms for the calcination products at 200, 400 and 800°C of ErOx.

accounts for the overall conversion of ErOx·$6H_2O$ to $Er_2O_2CO_3$ (expected ML is 39.6%). The similarity of the activation energy values (Table 1) for Processes IV and V justifies their overlapping. Hussein et al. [19] studied the thermal decomposition of holmium oxalate hydrate, nonisothermally in air, and reported that the marked similarity of the activation energy values justifies their overlapping.

The IR-gas-phase spectrum at 450°C (Fig. 2) shows an increase in CO_2. The IR-spectrum of ErOx-400 (Fig. 3) shows absorptions at 1660, 1525, 1390, 1070, and 850 cm^{-1} assignable to oxycarbonate species [17–20]. The strong absorption appearing at 700–500 cm^{-1} are related to Er–O vibrational modes [20]. The XRD pattern for the solid calcination (decomposition) product of ErOx at 400°C (ErOx-400), Fig. 4, reveals that the $Er_2O_2CO_3$ product inferred from the TG and IR data is amorphous.

As the temperature increases to 600°C, Process VI takes place endothermally. Process VI brings the total ML to 45.1% which is close to that calculated theoretically (45.4%) for the overall conversion of $Er_2(C_2O_4)_3{\cdot}6H_2O$ into Er_2O_3.

This is confirmed by the XRD pattern of ErOx800 shown in Fig. 4 which shows a single pattern of diffraction peaks characteristic of crystalline Er_2O_3 (ASTM No. 8-50). The IR-spectrum of ErOx-800 (Fig. 3) shows no detectable absorptions due to oxycarbonate species. The absorptions below 700 cm^{-1} are related to lattice vibration modes of Er_2O_3 [20]. The weak bands around 1600, 1530, and 1419 cm^{-1} are most probably due to surface contamination by carbonate and moisture since it is known that Er_2O_3 is a basic oxide [7]. Table 1 indicates that Process VI has the highest activation energy (160 kJ/mol) in the overall decomposition of ErOx·$6H_2O$.

It must be noted that the air atmosphere has shifted the decomposition steps to lower temperatures. It is known that the presence of oxygen accelerates the decomposition of carbonates and oxycarbonates [12,14].

4. Conclusions

1. The thermal decomposition of ErOx in air to form Er_2O_3 involves the following stages:

$$Er_2(C_2O_4)_3\cdot 6H_2O \quad (90°C) \rightarrow Er_2(C_2O_4)_3\cdot 3H_2O \qquad \text{(Step I)}$$

$$Er_2(C_2O_4)_3\cdot 6H_2O \quad (150°C) \rightarrow Er_2(C_2O_4)_3\cdot 2H_2O \qquad \text{(Step II)}$$

$$Er_2(C_2O_4)_3\cdot 6H_2O \quad (360°C) \rightarrow Er_2(C_2O_4)_3 \quad \text{(Step III)}$$

$$Er_2(C_2O_4)_3\cdot 6H_2O \quad (420°C) \rightarrow Er_2(CO_3)_3 \quad \text{(Step IV)}$$

$$Er_2(C_2O_4)_3\cdot 6H_2O \quad (450°C) \rightarrow Er_2O_2CO_3 \quad \text{(Step V)}$$

$$Er_2(C_2O_4)_3\cdot 6H_2O \quad (615°C) \rightarrow Er_2O_3 \quad \text{(Step VI)}$$

2. The lower hydrate oxalate (dihydrate) is thermally stable, but the anhydrous oxalate is unstable.
3. The dehydration processes are not affected by the nature of the atmosphere. The water of hydration is responsible for the crystal coherency.
4. $Er_2(CO_3)_3$ and $Er_2O_2CO_3$ are formed during the decomposition of ErOx, but as amorphous and unstable intermediates.
5. Nitrogen atmosphere has no effect on the decomposition pathway, but it shifts the decomposition temperatures to slightly higher values.

References

[1] A.K. Galwey, S.G. Mckee, T.R.B. Mitchell, M.E. Brown, A.F. Bean, Reactivity of Solids 6 (1988) 173.
[2] B. Delmon, P. Grange, P.A. Jacobs, G. Poncelet (Eds.), Preparation of Catalysts II, Elsevier, Amsterdam, 1970.
[3] M.E. Brown, D. Dollimore, A.K. Galwey, in: C.H. Bamford, C.F.H. Tipper (Eds.), Chemical Kinetics, Reactions in the Solid State, Vol. 22, Elsevier, Amsterdam, 1980, p. 130.
[4] P. Kofstad, Nonstoichiometry, Diffusion and Electrical Conductivity in Binary Metal Oxides, Wiley, New York, 1972.
[5] G.A.M. Hussein, J. Anal. Appl. Pyrolysis 37 (1996) 111.
[6] H. Arakawa, Techno Japan 21 (1988) 32.
[7] K. Tanabe, K. Mismo, Y. Ono, H. Hattori, New Solid Acids and Bases, Kodansha, Tokyo, Elsevier, NY, 1989.
[8] L.M. Dassuncao, I. Giolito, M. Ionashiro, Thermochim. Acta 137 (1989) 319.
[9] W. Brzyska, A. Krol, Thermochim. Acta 182 (1991) 293.
[10] K. Muraishi, H. Yokobayeshi, K. Nagase, Thermochim. Acta 182 (1991) 209.
[11] W. Brzyska, M. Sikorska, Pol. J. Chem. 66 (1992) 253.

[12] G.A.M. Hussein, J. Chem. Soc., Faraday Trans. 91 (1995) 1385.
[13] J.H. Flynn, J. Therm. Anal. 27 (1983) 45.
[14] G.A.M. Hussein, J. Phys. Chem. 98 (1994) 9657.
[15] J.V. Smith (Ed.), X-Ray Powder Data File, American Society for Testing and Materials, Philadelphia, USA, 1960.
[16] K. Nakamoto, Infrared Spectra of Inorganic and Coordination Compounds, Wiley, New York, 1970, p. 253.
[17] G.A. Gadsden, Infrared Spectra of Minerals and Related Inorganic Compounds, Butterworths, London, 1975, p. 65.
[18] G.A.M. Hussein, Thermochim. Acta 186 (1991) 187.
[19] G.A.M. Hussein, A.K. Nohman, M.I. Zaki, New J. Chem. 19 (1995) 77.
[20] J.A. Goldsmith, S.D. Ross, Spectrochem. Acta (A) 23 (1967) 1909.